jove

Interrogating Cell-Cell Interactions in the Salivary Gland *via Ex Vivo* Live Cell Imaging

Sonia Elder[1], **Justyna Cholewa-Waclaw**[1], **Elaine Emmerson**[1]

[1] The Centre for Regenerative Medicine, Institute for Regeneration and Repair, The University of Edinburgh

Corresponding Author

Elaine Emmerson
Elaine.Emmerson@ed.ac.uk

Citation

Elder, S., Cholewa-Waclaw, J., Emmerson, E. Interrogating Cell-Cell Interactions in the Salivary Gland *via Ex Vivo* Live Cell Imaging. *J. Vis. Exp.* (201), e65819, doi:10.3791/65819 (2023).

Date Published

November 17, 2023

DOI

10.3791/65819

URL

jove.com/video/65819

Abstract

Salivary gland regeneration is a complex process involving intricate interactions among various cell types. Recent studies have shed light on the pivotal role played by macrophages in driving the regenerative response. However, our understanding of this critical role has primarily relied on static views obtained from fixed tissue biopsies. To overcome this limitation and gain insights into these interactions in real time, this study outlines a comprehensive protocol for culturing salivary gland tissue *ex vivo* and capturing live images of cell migration.

The protocol involves several key steps: First, mouse submandibular salivary gland tissue is carefully sliced using a vibratome and then cultured at an air-liquid interface. These slices can be intentionally injured, for instance, through exposure to radiation, to induce cellular damage and trigger the regenerative response. To track specific cells of interest, they can be endogenously labeled, such as by utilizing salivary gland tissue collected from genetically modified mice where a particular protein is marked with green fluorescent protein (GFP). Alternatively, fluorescently-conjugated antibodies can be employed to stain cells expressing specific cell surface markers of interest. Once prepared, the salivary gland slices are subjected to live imaging using a high-content confocal imaging system over a duration of 12 h, with images captured at 15 min intervals. The resulting images are then compiled to create a movie, which can subsequently be analyzed to extract valuable cell behavior parameters. This innovative method provides researchers with a powerful tool to investigate and better understand macrophage interactions within the salivary gland following injury, thereby advancing our knowledge of the regenerative processes at play in this dynamic biological context.

Introduction

Macrophages have been shown to play increasingly important roles in the processes of regeneration and repair, extending beyond their classical immune function[1,2]. Indeed, macrophages are involved in a plethora of processes related to regeneration, exhibiting critical regulatory activity in all stages of repair, as well as scar formation and fibrosis[3,4]. Tissue-resident macrophages are highly heterogeneous cell types with complex mechanisms driving diverse cellular phenotypes, and they play essential roles in organ development, function, and homeostasis (as reviewed in[5]). Tissue-resident macrophages initially arise from precursors in the yolk sac and fetal liver, and they are subsequently replaced by proliferation or by bone marrow-derived blood monocytes at varying rates, depending on the longevity of existing macrophages and the tissue or niche within which they reside[6,7].

Importantly, tissue-resident macrophages are dispersed throughout all tissues and contribute to diverse organ functions. They are uniquely programmed by their microenvironment to perform niche-specific functions. For this reason, the localization of macrophages within the tissue offers insight into their function, with unique populations observed in the lung, mammary gland, intestine, skin, and muscle[8,9,10]. During mammary gland development, ductal macrophages are intimately associated with the ductal tree, and their depletion results in significantly reduced branching[11]. Furthermore, macrophages are required for morphogenesis during puberty and alveologenesis in pregnancy, where they actively monitor the epithelium. In muscle injury, a specific population of macrophages "dwells" within the injury site, providing a transient niche in which they supply proliferation-induced cues required for stem cell proliferation. Thus, they exhibit the specialized role of distinct macrophage populations in governing the repair process[2]. In the lung, a similar phenomenon occurs where interstitial macrophages prime interleukin (IL)-R1-expressing alveolar type II (AT2) cells for conversion into damage-associated transient progenitors through the release of IL-1B[12]. Furthermore, recent research has shown that macrophages are essential for the regeneration of the mouse submandibular salivary gland (SMG) after irradiation injury, and in their absence, epithelial regeneration is disrupted[13]. Taken together, this data highlights the importance of macrophage activation and function in transient inflammatory niches after tissue injury, as well as during homeostasis.

Macrophages are active cells, and their functions involve interactions with a variety of different cell types, including direct cell-cell contact[14,15], as well as more indirect methods such as the secretion of soluble factors[2,16], which are essential for niche regulation. While classical immunofluorescent imaging is useful to begin unraveling these interactions, it is limited by depicting only a single snapshot in time, thereby omitting numerous timepoints critical to a highly dynamic regenerative process[17,18]. As the importance of timing and the emergence of different waves of regeneration come into sharper focus, it is essential to dissect these processes in greater detail.

Radiotherapy is a life-saving treatment for many people diagnosed with cancer. While often effective at shrinking or eliminating the tumor(s), radiotherapy can also damage healthy tissues lying in the radiation field and elicit an immune response. Radiation injury can induce rapid macrophage recruitment, and direct and indirect immunomodulatory

responses[19,20]. The salivary glands are often inadvertently irradiated during treatment for head and neck cancer[21,22], leading to epithelial damage, cell atrophy, and fibrosis[23,24], resulting in xerostomia or chronic dry mouth[25].

The salivary gland is composed of a plethora of cell types and structures, including but not limited to epithelial cells (both saliva-producing acinar cells and saliva-transporting ductal cells), myoepithelial cells, epithelial progenitor cells, nerves, blood vessels, immune cells, fibroblasts, and extracellular matrix (ECM). The role and response of many of these cell types in the regenerative response have been previously described[26,27,28,29,30]. However, how these different cells interact during homeostasis and regeneration, and particularly how immune cells such as macrophages behave, is less well studied. This manuscript describes a newly established method to study the live interactions between SMG macrophages and other cells of interest in *ex vivo* tissue. The SMG is sliced on a vibratome, stained for surface markers, and imaged for up to 12 h. Using this method, phagocytosis of surrounding cells by macrophages can be observed, macrophage migration kinetics can be studied, and direct cell-cell interactions between macrophages and epithelial cells can be demonstrated.

Protocol

All procedures were approved by the UK Home Office and performed under PPLs PB5FC9BD2 and PP0330540. All experiments align to ARRIVE guidelines and those of the University of Edinburgh.

Wild-type mice were commercially obtained (see **Table of Materials**). *Krt14*$^{CreER;}$ R26^{mTmG} mice were bred in house, by crossing *Krt14*$^{CreER/+}$ mice[31] with *R26*$^{mTmG/\ mTmG}$ mice[32]. In all experiments, female 8-10 week old mice were used.

1. Collecting and embedding the SMG

1. Euthanize the mouse/mice by exposing them to a rising concentration of carbon dioxide (CO_2). Afterward, spray the incision area with 70% ethanol (EtOH) and use scissors and forceps to carefully dissect the SMG(s) from the surrounding tissue (**Figure 1A**). Remove any fat and connective tissue using forceps, and place the gland in a collection tube containing ice-cold Hanks Balanced Salt Solution (HBSS, see **Table of Materials**).
2. Separate the gland into pieces measuring approximately 1 cm^2 each using forceps.
3. Heat 4% agarose to 50 °C, and then pour it directly into a 35 mm dish.
4. Pour a small amount of melted 50 °C agarose into a separate dish and thoroughly rinse the gland by moving it around in the excess agarose.
   NOTE: This step is necessary to remove excess liquid from the glands. An excess of liquids can prevent the glands from adhering properly to the agarose.
5. Position 4-6 pieces of the gland into the agarose, ensuring that they lie flat and are in the same plane (**Figure 1A**).
   NOTE: Ensure the glands do not touch the surface of the agar or the bottom of the plate.
6. Place the lid on the 35 mm dish and transfer it to an icebox, covering the plate with ice.
7. Wait for 5-10 min for the agarose to solidify.

2. Sectioning

1. Use a scalpel to carefully cut around the gland-embedded agarose block, removing the block containing the tissue from the dish. Leave approximately a 5 mm border.
2. Attach the agarose block to the stage of the vibratome (see **Table of Materials**) by applying a drop of superglue, ensuring that the entire bottom surface of the block is in contact with the superglue.
3. Allow the superglue to harden for approximately 5 min. Then, fill the vibratome chamber with ice-cold 1x phosphate-buffered saline (PBS) containing 1% Penicillin-Streptomycin (P/S).
4. Add ice to both the side and bottom of the vibratome chamber.
   NOTE: Maintain a very cold environment and replace the ice as needed.
5. Trim off any excess agarose and create 5 mm gaps between each piece of gland by making incisions with a scalpel. This will yield individual slices.
6. Align the vibratome blade with the face of the agarose block and set the start and end points of the sections to achieve the desired slice thickness.
7. Before starting the cutting process, ensure that the blade is not in contact with the block. This precaution will prevent accidentally cutting large pieces of agarose and losing parts of the sample.
8. Cut sections with a thickness of 150 µm at a low speed and high vibration (e.g., a speed of 3 and a vibration setting of 8-10 on a scale of 1-10 for each parameter) (**Figure 1A**).
9. Once a section is cut and released into the surrounding PBS, collect the sections using a paintbrush and place them in a dish containing pre-warmed Roswell Park Memorial Institute (RPMI) media with P/S.

3. Culturing and staining of SMG slices

1. Culturing
   1. Add 1.5 mL of RPMI media to each well of a 6-well plate that contains a 0.4 µm filter. Ensure there are no air bubbles trapped underneath the filter.
   2. Transfer 1-6 slices onto each filter using a paintbrush, taking care not to break the slices.
      NOTE: Ensure that the slices are not submerged in media but are instead floating on the filter. If they are fully submerged, they may suffocate during culture.
   3. Incubate at 37 °C with 5% CO_2, and change the media every 3 days (**Figure 1A**).
   4. Irradiate experimental plates with a single dose of 10 Gy gamma radiation using a commercially available irradiator (see **Table of Materials**). Afterward, return them to the incubator.
2. Staining for live imaging
   1. Using a paintbrush, gently lift the slices from the filter and place them into a 24-well plate containing 500 µL of culture media per well, where the slices will be submerged.
   2. Add the relevant conjugated antibodies and nuclear stain (see **Table of Materials**) to the media at the appropriate concentrations[27].
   3. Incubate the slices with antibodies for 2 h at 37 °C with gentle agitation.

4. Wash the slices by submerging them in culture media and washing for 3 rounds of 10 min washes at 37 °C with gentle agitation.

4. Mounting and live imaging

1. Using forceps, remove the tape from one side of a double-sided imaging spacer and adhere it, adhesive side down, to the bottom of a glass-bottom 6-well plate.
2. Pipette 50 µL of media into the gap in the center of the spacer.
3. Place the slice into the media using a paintbrush, ensuring that it lies flat without any trapped air bubbles.
4. Using a pipette, carefully remove 20 µL of media from the gap.
5. Remove the tape from the top side of the spacer using forceps and place a 25 mm circular coverslip on top. Press around the edge of the spacer to ensure that the coverslip firmly attaches, being cautious not to break the coverslip by applying too much force (**Figure 1A**).
6. Image the slice on a confocal microscope for the desired time period or intervals (e.g., every 15 min for 12 h using a 20x water objective).

Representative Results

The response of macrophages to injury in the submandibular salivary gland remains unknown. This includes whether they localize and migrate to specific structures within the gland, as well as the distance and speed at which they migrate. This has been difficult to determine through static imaging approaches.

To address this, a live imaging approach to study macrophage-epithelial cell interaction in real-time has been developed. Immunofluorescent staining of slices was combined with an endogenously labeled lineage-tracing mouse model (**Figure 1A** and **Figure 2A**). In this model, slices were exposed to 10 Gy of gamma irradiation to induce irradiation injury and were imaged at 2 h, 3 days, and 4 days post-irradiation (IR), with non-irradiated slices serving as controls. Data were acquired from four channels: Hoechst (using laser 425 to minimize phototoxicity), GFP (488), dTomato (561), and Alexa 647 (640). A z-stack was performed, and an image was captured every 2-3 µm, with a total of 30 to 40 planes collected, resulting in an overall height of 80-90 µm.

Using this technique and analyzing membrane-bound Tomato (mT) signal and Caspase3/7 activity, it became evident that organotypic slices retained their epithelial structure, survived in culture, and exhibited minimal cell death. The data showed that non-irradiated slices of the submandibular gland from *R26*^{mTmG} mice[32], cultured for 7 days, retained their mT signal and epithelial architecture (**Figure 1B**). However, at 3 days following *ex vivo* irradiation, acinar and ductal cell atrophy was evident (**Figure 1B**; acini and ductal structures highlighted by dashed white and green lines, respectively), consistent with *in vivo* radiation injury[13]. Apoptosis was negligible in the non-irradiated slices, but there was evidence of Caspase 3/7^{+} cells in the irradiated slices at 4 days post-irradiation (**Figure 1C**; green arrows), similar to *in vivo* injury[33,34]. Furthermore, irradiated slices recapitulated *in vivo* DNA damage[34,35,36,37], as indicated by elevated γH2AX[38] compared to non-irradiated controls (**Figure 1D,E**). Thus, organotypic salivary gland slices exhibited good viability in culture and responded similarly to *in vivo* tissue to irradiation.

Following this, real-time cell-cell interactions were investigated. Macrophages directly interacting with

GFP-labeled epithelial progenitor cells (*Krt14*$^{CreER\text{-}GFP}$) were observed over a 12 h time period at 3 days post-IR (**Figure 2A** and **Video 1**). Remarkably, it was evident that macrophages remained in close proximity to epithelial progenitor cells for hours, often staying in contact for the entire 12 h imaging period. Furthermore, real-time phagocytosis of epithelial cells by macrophages was observed, confirming that macrophages carry out their traditional function in the slice culture model (**Figure 2B**, **Videos 2** and **Video 3**). This technique also identified that macrophages are relatively stationary during both homeostasis and following irradiation injury, likely due to their high density within the tissue. This demonstrates, for the first time, that salivary gland macrophages do not migrate extensively during homeostasis or after irradiation injury. However, while macrophages did not show significant migration, the surrounding tissue displayed increased dynamics following irradiation, with multiple macrophages actively interacting around clusters of labeled epithelial cells. Additionally, based solely on nuclear staining, this technique allowed us to visualize cell movement within the slice over time, often with entire ducts appearing to 'migrate' within the tissue (**Video 4**). Over time during the culturing process, it became evident that slices shifted from a flat to a spheroid-like morphology, suggesting that cell movement within the slice is likely due to their rearrangement into a sphere-like structure, resembling a potential reorganization event.

Finally, the live imaging data generated by this assay can be used to quantitatively measure cell behavior, such as migration. Individual cells can be detected and segmented (**Figure 3A**), and migration can be measured using a commercially available imaging and analysis software (see **Table of Materials** and **Video 5**). Furthermore, nearest object analysis can be undertaken to determine whether cells, in this case, macrophages, migrate closer to other cells of interest, in this case, *Krt14*$^{CreER\text{-}GFP+}$ cells, and how this dynamic changes over time (**Figure 3B**).

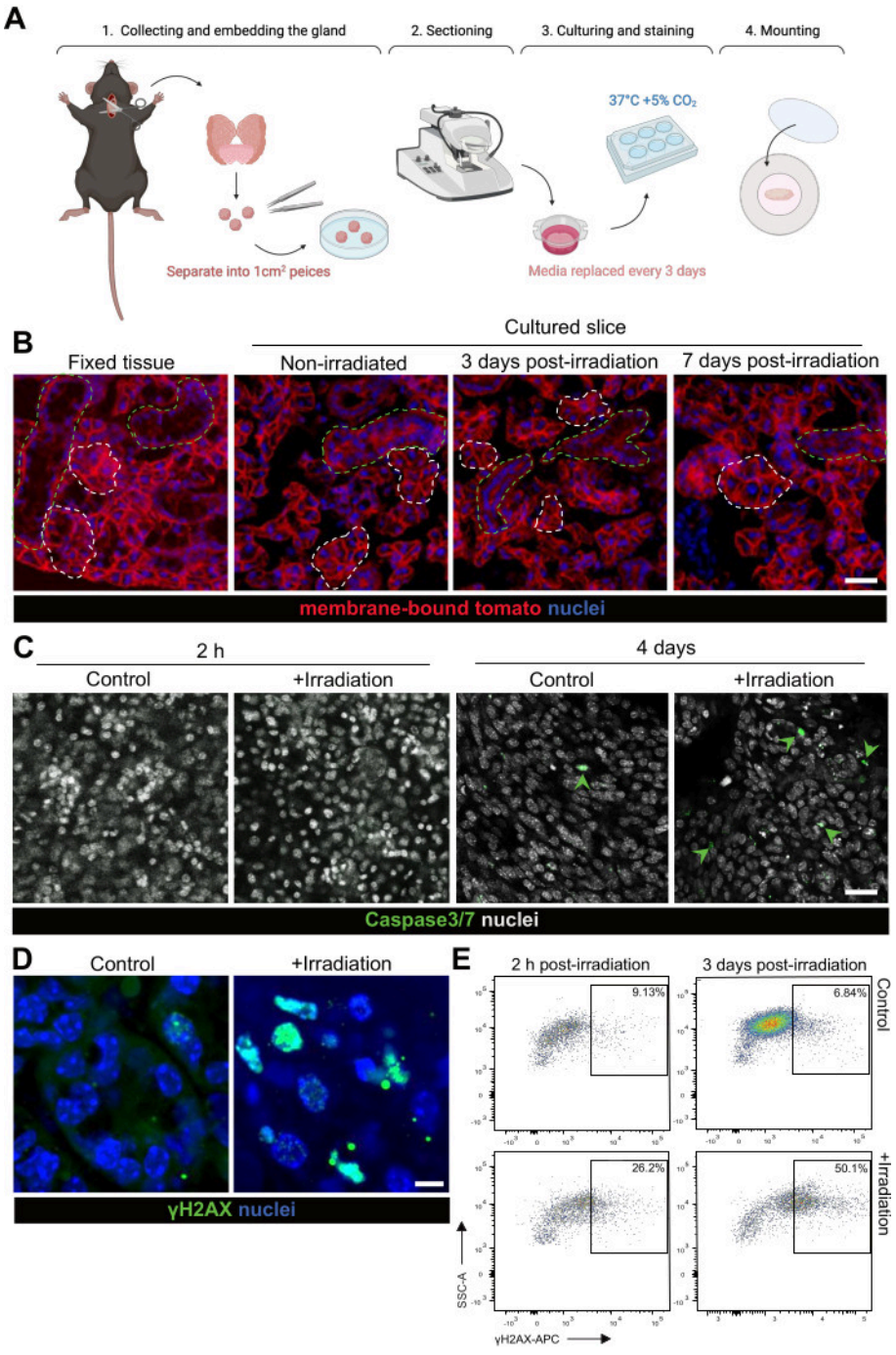

Figure 1: Recapitulation of *in vivo* response in precision-cut salivary gland tissue slices. (**A**) Schematic of the experimental protocol. (**B**) Representative images of membrane-bound Tomato obtained from fresh submandibular gland (SMG) tissue, unmanipulated SMG slices cultured for 7 days, or SMG slices irradiated with a single dose of 10 Gy gamma irradiation 3 or 7 days earlier. Dashed white lines indicate example acinar structures, and dashed green lines indicate example ductal structures. Scale bar = 50 µm. (**C**) Representative images of Caspase-3/7 expression obtained from

unmanipulated SMG slices or SMG slices irradiated with a single dose of 10 Gy gamma irradiation 2 h or 4 days earlier. Green arrowheads indicate positive nuclei. Scale bar = 50 µm. (**D**) Representative images of γH2AX expression obtained from unmanipulated SMG slices or SMG slices irradiated with a single dose of 10 Gy gamma irradiation 3 days earlier. Scale bar = 20 µm. (**E**) Representative expression of γH2AX in $EpCAM^{+}$ epithelial cells from unmanipulated SMG slices or SMG slices irradiated with a single dose of 10 Gy gamma irradiation 2 h and 3 days earlier. SSA = side scatter area. Please click here to view a larger version of this figure.

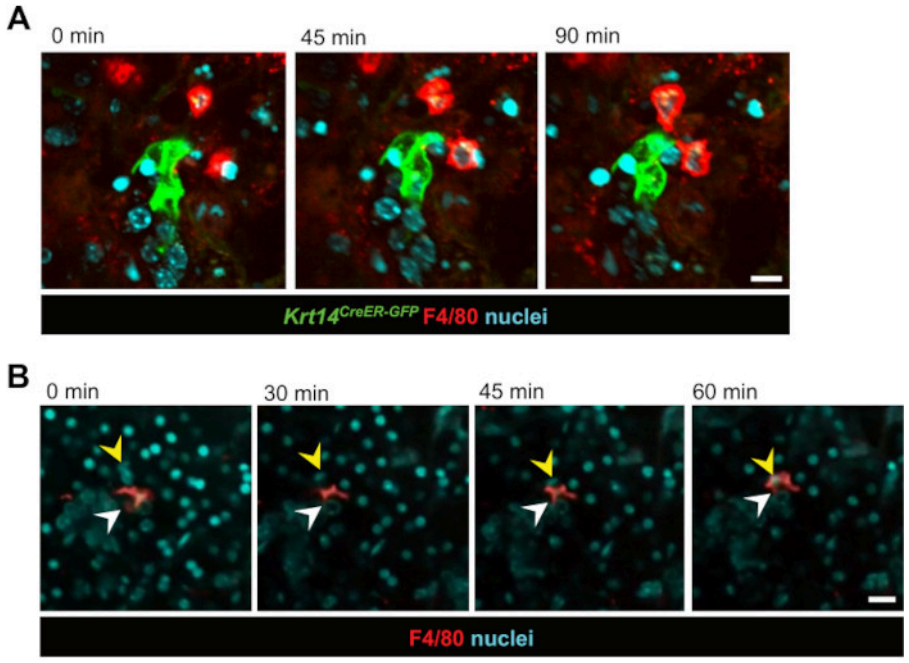

Figure 2: Live imaging of macrophage-epithelial cell interactions and phagocytosis. (**A**) Sequential still images of interactions between KRT14+ progenitor cells and their progeny (*Krt14*$^{CreER\text{-}GFP+}$ cells) and macrophages following irradiation. Live cell imaging captures cellular dynamics over a 90 min period. Scale bar = 20 µm. Associated video is **Video 1**. (**B**) Sequential still images of a macrophage phagocytosing an epithelial cell. Live cell imaging shows the process over a 60 min period. White arrows point to the macrophage, and yellow arrows indicate the nucleus of the cell undergoing phagocytosis. Scale bar = 50 µm. Associated video is **Video 2**. Please click here to view a larger version of this figure.

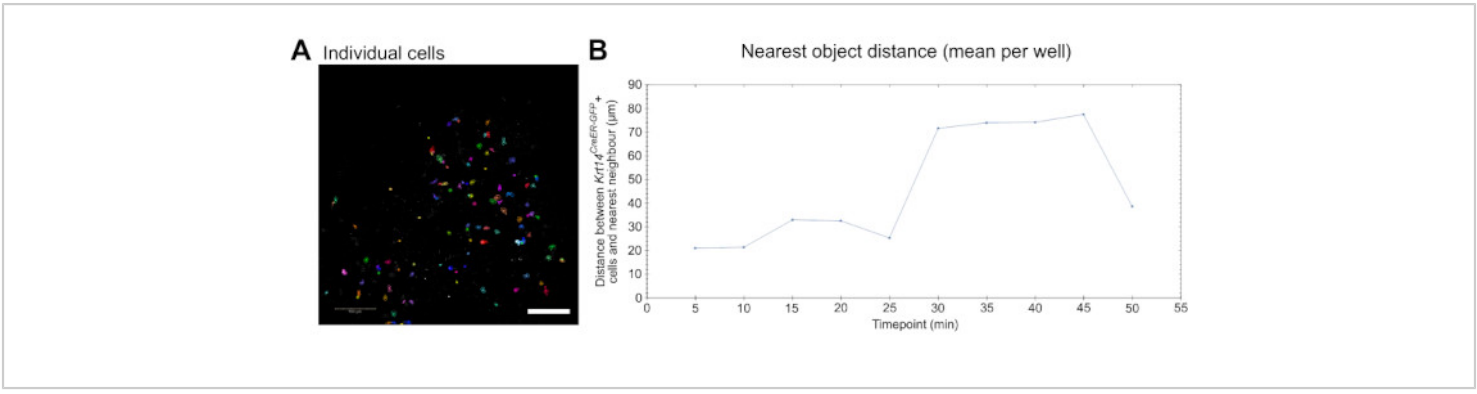

Figure 3: Live imaging for cellular dynamics analysis. (**A**) Image illustrating individual cell identification and segmentation for analyzing cellular behavior parameters, such as migration (see **Video 5**). Cells are pseudocolored randomly for individual cell and track distinction. Scale bar = 100 µm. (**B**) Quantification of the distance (in µm) of the nearest object to individual *Krt14*$^{CreER\text{-}GFP+}$ cells plotted over 10 time points (images captured every 5 min). Data presented as the mean value per well. Please click here to view a larger version of this figure.

Video 1: Live imaging revealing dynamic interactions between KRT14+ progenitor cells/progeny and macrophages after irradiation. Slices were exposed to a single 10 Gy gamma irradiation dose before live imaging. *Krt14*$^{CreER\text{-}GFP+}$ cells are represented in green, macrophages (F4/80+) in red, and nuclei in cyan. The video comprises a single z-stack, spanning a 12 h culture period with images captured every 15 min. Please click here to download the video.

Video 2: Live imaging capturing a macrophage engulfing an epithelial cell. Macrophages (F4/80+) are depicted in red, and nuclei are shown in cyan. The video consists of a single z-stack and spans a 12 h culture period with images taken every 15 min.Please click here to download the video.

Video 3: Maximum projection live imaging showing a macrophage engulfing an epithelial cell. Macrophages (F4/80+) are displayed in red, and nuclei are shown in cyan. The video features a maximum projection of z-stack images totaling 80 µm (a single plane is presented in **Video 2**) and spans a 12 h culture period with images taken every 15 min.Please click here to download the video.

Video 4: Live imaging illustrating the dynamic behavior of salivary gland epithelium in culture after irradiation. Slices were subjected to a single 10 Gy gamma irradiation dose before live imaging. Macrophages (F4/80+) are represented in red, nuclei in cyan. The video comprises a single z-stack, spanning a 12 h culture period with images captured every 15 min.Please click here to download the video.

Video 5: Quantitative cell migration tracking over time. This video demonstrates the individual tracing of cell tracks from live imaging videos. Arrows indicate cell tracks, and cells are pseudo-colored individually. The video consists of a single z-stack and spans a 1 h culture period with images taken every 15 min.Please click here to download the video.

Discussion

The ability to culture salivary gland tissue *ex vivo* presents an excellent opportunity to study cell-cell interactions in the context of both homeostasis and injury response. Although intravital imaging of the mouse submandibular gland is feasible[39,40], this technique depends on using fluorescent reporter mouse models to endogenously label cells of interest and must be performed under terminal anesthesia. Here, a method to culture submandibular gland slices *ex vivo* is described, maintaining cellular architecture and cell-cell interactions. This approach refines current live imaging techniques and provides an alternative to intravital imaging.

The long-term maintenance of tissue using this technique relies on culturing slices at an air-liquid interface. Previous explant models[26,41] have likely achieved successful culture for only a few days because they were submerged in media and essentially "suffocated." In contrast, the use of an air-liquid interface culture system maintains tissue health and structure for an extended period, ensuring high-quality imaging. The method of mounting SMG slices before imaging, with a small amount of media and within a space-restricted chamber to keep the slice flat, is integral to the technique's success. Visualization of cells in this assay depends on endogenously labeled reporter mice or fluorescently-conjugated antibodies. The abundance of transgenic fluorescent reporter mouse models and conjugated antibodies targeting specific cell types and subsets makes this method suitable for exploring various cell-specific interactions.

While this method provides a good model of tissue *in situ* and *ex vivo* irradiation injury results in acinar and ductal structure atrophy, similar to what occurs *in vivo*[13], some elements cannot be recapitulated *ex vivo*. These include the lack of functioning vasculature and neuronal input, as well as the absence of infiltrating inflammatory cells. Given the well-documented role of blood vessels and nerves in salivary gland homeostasis and regeneration[26,42] and the importance of migratory immune cells[43], such as T and B cells, in salivary gland function, injury response, infection, and Sjögren's Syndrome (SS) pathogenesis (as reviewed in[44]), this assay may miss some important cellular interactions. Additionally, very fast migratory events, such as Natural Killer (NK) cell[45] and Dendritic Cell (DC)[46] movement, may be missed by imaging every 15 min. However, imaging intervals can be optimized to study the specific cell-cell interactions of interest, and the ability to image in 3 dimensions through z-stacks allows the assessment of 3D cell movement. Securely mounting the tissue during imaging is crucial for quantification, such as cell tracking measurements. Furthermore, although this study utilized mouse tissue, the protocol provides a viable method for studying cell-cell interactions in human salivary glands, generating valuable translational information unattainable through other methods.

While the role of tissue-resident macrophages in homeostasis and regeneration has been demonstrated in several tissues[2,10,11,12], their role in the salivary glands remains largely unanswered. Although it is known that macrophages are essential for epithelial regeneration after irradiation injury[13], the precise mechanisms underlying this effect remain unknown. Live imaging of salivary gland slices enables real-time visualization and analysis of complex tissue dynamics, which are often missed by traditional confocal imaging. Additionally, it is evident that macrophages undergo dynamic changes in shape while performing various functions *in vivo*[47,48,49], and this protocol likely provides a better representation of these changes than a typical static view in fixed tissue. Future studies can utilize this technique to

investigate how cell-cell communication changes across the course of homeostasis, injury, and regeneration/resolution. This approach will be useful for elucidating key signaling pathways and events that may ultimately offer therapeutic benefits.

Disclosures

The authors have no conflicts of interest to disclose.

Acknowledgments

SE is funded by Wellcome Trust grant 108906/Z/15/Z; EE is funded by UKRI/MRC grant MR/S005544/1 and by a Chancellor's Fellowship from the University of Edinburgh. Figure 1A is created with BioRender.com.

References

1. Wynn, T. A., Vannella, K. M. Macrophages in tissue repair, regeneration, and fibrosis. *Immunity.* **44** (3), 450-462 (2016).
2. Ratnayake, D. et al. Macrophages provide a transient muscle stem cell niche via NAMPT secretion. *Nature.* **591** (7849), 281-287 (2021).
3. Lucas, T. et al. Differential roles of macrophages in diverse phases of skin repair. *J Immunol.* **184** (7), 3964-3977 (2010).
4. Duffield, J. S. et al. Selective depletion of macrophages reveals distinct, opposing roles during liver injury and repair. *J Clin Invest.* **115** (1), 56-65 (2005).
5. Wynn, T. A., Chawla, A., Pollard, J. W. Macrophage biology in development, homeostasis and disease. *Nature.* **496** (7446), 445-455 (2013).
6. Ginhoux, F., Schultze, J. L., Murray, P. J., Ochando, J., Biswas, S. K. New insights into the multidimensional concept of macrophage ontogeny, activation and function. *Nat Immunol.* **17** (1), 34-40 (2016).
7. Mass, E., Nimmerjahn, F., Kierdorf, K., Schlitzer, A. Tissue-specific macrophages: how they develop and choreograph tissue biology. *Nat Rev Immunol.* **23** (9), 563-579 (2023).
8. Dick, S. A. et al. Three tissue resident macrophage subsets coexist across organs with conserved origins and life cycles. *Sci Immunol.* **7** (67), eabf7777 (2022).
9. Hassel, C., Gausserès, B., Guzylack-Piriou, L., Foucras, G. Ductal macrophages predominate in the immune landscape of the lactating mammary gland. *Front Immunol.* **12** 754661 (2021).
10. Kolter, J. et al. A subset of skin macrophages contributes to the surveillance and regeneration of local nerves. *Immunity.* **50** (6), 1482-1497.e1487 (2019).
11. Dawson, C. A. et al. Tissue-resident ductal macrophages survey the mammary epithelium and facilitate tissue remodelling. *Nat Cell Biol.* **22** (5), 546-558 (2020).
12. Choi, J. et al. Inflammatory signals induce AT2 cell-derived damage-associated transient progenitors that mediate alveolar regeneration. *Cell Stem Cell.* **27** (3), 366-382.e367 (2020).
13. McKendrick, J. G. et al. CSF1R-dependent macrophages in the salivary gland are essential for epithelial regeneration after radiation-induced injury. *Sci Immunol.* **8** (89), eadd4374, doi:10.1126/sciimmunol.add4374, (2023).
14. Muntjewerff, E. M., Meesters, L. D., van den Bogaart, G. Antigen cross-presentation by macrophages. *Front Immunol.* **11**, 1276 (2020).

15. Bissonnette, E. Y., Lauzon-Joset, J. F., Debley, J. S., Ziegler, S. F. Cross-talk between alveolar macrophages and lung epithelial cells is essential to maintain lung homeostasis. *Front Immunol.* **11**, 583042 (2020).

16. Xue, Q. et al. Analysis of single-cell cytokine secretion reveals a role for paracrine signaling in coordinating macrophage responses to TLR4 stimulation. *Sci Signal.* **8** (381), ra59 (2015).

17. McArdle, S., Mikulski, Z., Ley, K. Live cell imaging to understand monocyte, macrophage, and dendritic cell function in atherosclerosis. *J Exp Med.* **213** (7), 1117-1131 (2016).

18. Gurevich, D. B. et al. Live imaging of wound angiogenesis reveals macrophage orchestrated vessel sprouting and regression. *Embo j.* **37** (13), e97786 (2018).

19. Meziani, L. et al. CSF1R inhibition prevents radiation pulmonary fibrosis by depletion of interstitial macrophages. *Eur Respir J.* **51** (3), 1702120 (2018).

20. Bickelhaupt, S. et al. Effects of CTGF blockade on attenuation and reversal of radiation-induced pulmonary fibrosis. *J Natl Cancer Inst.* **109** (8), djw339 (2017).

21. Formenti, S. C., Demaria, S. Systemic effects of local radiotherapy. *Lancet Oncol.* **10** (7), 718-726 (2009).

22. Chambers, M. S., Garden, A. S., Kies, M. S., Martin, J. W. Radiation-induced xerostomia in patients with head and neck cancer: pathogenesis, impact on quality of life, and management. *Head Neck.* **26** (9), 796-807 (2004).

23. Radfar, L., Sirois, D. A. Structural and functional injury in minipig salivary glands following fractionated exposure to 70 Gy of ionizing radiation: an animal model for human radiation-induced salivary gland injury. *Oral Surg Oral Med Oral Pathol Oral Radiol Endod.* **96** (3), 267-274 (2003).

24. Grehn, A. L., Gustafsson, H., Franzén, L., Thornell, L. E., Henriksson, R. Ultrastructural morphometry of parotid acinar cells following fractionated irradiation. *Oral Oncol.* **33** (1), 23-28 (1997).

25. Rocchi, C., Emmerson, E. Mouth-watering results: clinical need, current approaches, and future directions for salivary gland regeneration. *Trends Mol Med.* **26** (7), 649-669 (2020).

26. Emmerson, E. et al. Salivary glands regenerate after radiation injury through SOX2-mediated secretory cell replacement. *EMBO Mol Med.* **10** (3), e8051 (2018).

27. May, A. J. et al. Diverse progenitor cells preserve salivary gland ductal architecture after radiation-induced damage. *Development.* **145** (21), dev166363 (2018).

28. Knox, S. M. et al. Parasympathetic stimulation improves epithelial organ regeneration. *Nat Commun.* **4**, 1494 (2013).

29. Mizrachi, A. et al. Radiation-induced microvascular injury as a mechanism of salivary gland hypofunction and potential target for radioprotectors. *Radiat Res.* **186** (2), 189-195 (2016).

30. Friedrich, R. E., Bartel-Friedrich, S., Holzhausen, H. J., Lautenschläger, C. The effect of external fractionated irradiation on the distribution pattern of extracellular matrix proteins in submandibular salivary glands of the rat. *J Craniomaxillofac Surg.* **30** (4), 246-254 (2002).

31. Vasioukhin, V., Degenstein, L., Wise, B., Fuchs, E. The magical touch: genome targeting in epidermal stem cells induced by tamoxifen application to mouse skin. *Proc Natl Acad Sci U S A.* **96** (15), 8551-8556 (1999).

32. Muzumdar, M. D., Tasic, B., Miyamichi, K., Li, L., Luo, L. A global double-fluorescent Cre reporter mouse. *Genesis.* **45** (9), 593-605 (2007).

33. Gilman, K. E. et al. P2X7 receptor deletion suppresses γ-radiation-induced hyposalivation. *Am J Physiol Regul Integr Comp Physiol.* **316** (5), R687-r696 (2019).

34. Ren, J. et al. Radioprotective effects and mechanism of HL-003 on radiation-induced salivary gland damage in mice. *Sci Rep.* **12** (1), 8419 (2022).

35. Marmary, Y. et al. Radiation-induced loss of salivary gland function is driven by cellular senescence and prevented by IL6 modulation. *Cancer Res.* **76** (5), 1170-1180 (2016).

36. Chang, S. et al. Inorganic nitrate alleviates total body irradiation-induced systemic damage by decreasing reactive oxygen species levels. *Int J Radiat Oncol Biol Phys.* **103** (4), 945-957 (2019).

37. Varghese, J. J. et al. Localized delivery of amifostine enhances salivary gland radioprotection. *J Dent Res.* **97** (11), 1252-1259 (2018).

38. Mah, L. J., El-Osta, A., Karagiannis, T. C. gammaH2AX: a sensitive molecular marker of DNA damage and repair. *Leukemia.* **24** (4), 679-686 (2010).

39. Takano, T. et al. Highly localized intracellular Ca(2+) signals promote optimal salivary gland fluid secretion. *Elife.* **10**, e66170 (2021).

40. Ficht, X., Thelen, F., Stolp, B., Stein, J. V. Preparation of murine submandibular salivary gland for upright intravital microscopy. *J Vis Exp.* **135**, e57283 (2018).

41. O'Dell, N. L., Sharawy, M. H., Schuster, G. S. Effects of *in vivo* single and multiple isoproterenol injections on subsequently explanted submandibular glands. *Acta Anat (Basel).* **105** (4), 431-438 (1979).

42. Lombaert, I. M. et al. Cytokine treatment improves parenchymal and vascular damage of salivary glands after irradiation. *Clin Cancer Res.* **14** (23), 7741-7750 (2008).

43. Stolp, B. et al. Salivary gland macrophages and tissue-resident CD8(+) T cells cooperate for homeostatic organ surveillance. *Sci Immunol.* **5** (46), eaaz4371 (2020).

44. Verstappen, G. M., Pringle, S., Bootsma, H., Kroese, F. G. M. Epithelial-immune cell interplay in primary Sjögren syndrome salivary gland pathogenesis. *Nat Rev Rheumatol.* **17** (6), 333-348 (2021).

45. Vanherberghen, B. et al. Microwell-based live cell imaging of NK cell dynamics to assess heterogeneity in motility and cytotoxic response. *Methods Mol Biol.* **1441**, 87-106 (2016).

46. de Winde, C. M., Munday, C., Acton, S. E. Molecular mechanisms of dendritic cell migration in immunity and cancer. *Med Microbiol Immunol.* **209** (4), 515-529 (2020).

47. Neupane, A. S. et al. Patrolling alveolar macrophages conceal bacteria from the immune system to maintain homeostasis. *Cell.* **183** (1), 110-125.e111 (2020).

48. Paterson, N., Lämmermann, T. Macrophage network dynamics depend on haptokinesis for optimal local surveillance. *Elife.* **11**, e75354 (2022).

49. Lim, K. et al. In situ neutrophil efferocytosis shapes T cell immunity to influenza infection. *Nat Immunol.* **21** (9), 1046-1057 (2020).